Mechanical and mineralogical characteristics of mortars with crushed and river sand

Emmanuel Elat, Alexandre Pierre, Prosper Pliya, Myriam Duc, Michel Mbessa, Albert Noumowe

▶ **To cite this version:**

Emmanuel Elat, Alexandre Pierre, Prosper Pliya, Myriam Duc, Michel Mbessa, et al.. Mechanical and mineralogical characteristics of mortars with crushed and river sand. The 13th fib International PhD-Symposium in Civil Engineering, Aug 2020, Marne-la-Vallée, France. pp. 78-85, graph., photos., bibliogr. hal-03113712v2

HAL Id: hal-03113712
https://hal.science/hal-03113712v2

Submitted on 6 Apr 2021

HAL is a multi-disciplinary open access archive for the deposit and dissemination of scientific research documents, whether they are published or not. The documents may come from teaching and research institutions in France or abroad, or from public or private research centers.

L'archive ouverte pluridisciplinaire **HAL**, est destinée au dépôt et à la diffusion de documents scientifiques de niveau recherche, publiés ou non, émanant des établissements d'enseignement et de recherche français ou étrangers, des laboratoires publics ou privés.

Mechanical and mineralogical characteristics of mortars with crushed and river sand

Emmanuel Elat[1,2,*], Alexandre Pierre[1], Prosper Pliya[1], Myriam Duc[3], Michel Mbessa[2], Albert Noumowé[1]

[1]Laboratory of Mechanics and Materials of Civil Engineering (L2MGC), CY Cergy Paris University, 5 Mail Gay-Lussac-Neuville sur Oise, F-95031 Cergy-Pontoise Cedex, France,
[2]Laboratory of Mechanics, Materials, Structures and Production, (LMMPS), National Advanced School of Engineering, University of Yaounde I: P.O Box 8390 Yaounde-Cameroon,
[3]University Gustave Eiffel, Laboratory Soils, Rocks and Geotechnical Structures, 14-20 boulevard Newton - Champs-sur-Marne, 77447 Marne-la-Vallée cedex 2, France

Abstract

The aim of this study is to characterize the mixtures of crushed sand and river sand for an optimal use in the formulation of mortars and concretes. Physical, chemical and mineralogical characterization of aggregates was done, followed by the formulation of mortars by substituting 100%, 50% and 0% of river sand by crushed sand. The compressive strength and the water porosity were measured on mortar specimens, completed by a microstructural characterization using XRD, DTG, and SEM examinations. The results showed that ettringite, CSH and portlandite contents are similar in tested mortar while a slight difference of carbonation appeared with a lower carbonation in crushed sand. Besides, 100% river sand mortar was highly porous, with low compressive strength at 28 days, compared to crushed sand mortars containing more fines, less porous and with better compressive strength.

Key words: crushed sand, alluvial sand, mortar, compressive strength, mineralogical characteristics

1 Introduction

River sand is a material widely used in the construction of civil engineering infrastructures. However, its extraction became expensive and limited because of environmental protection. In addition, some regions in the world are located far from rivers, which reinforces the search of sand from various origins. The use of crushed sand from quarries in the production of cementious materials is an analternative to reduce the overexploitation or to replace the river sand [1]. However, the use of crushed sand may have consequences on the mechanical behaviour and the durability of concretes [2]. Indeed, these sands present various characteristics compared to alluvial sands containing usually finer sized particles and with an adequate morphology to reduce the concrete porosity. These properties ensure granular continuity between cement and gravel for better cohesion of concrete [3].

In Cameroon, the exploitation of aggregate in quarries increased considerably in recent years, with the production of crushed sands. These sands are used in the manufacture of mortars and concretes, while the scientific recommendations on their use remained scarce. It explains the renewed interest in the influence of crushed sand on mortar properties.

Among literature, Menadi et al.[4] studied the strength and durability of concrete incorporating crushed limestone sand. The authors proved that up to 15% of fine content in crushed sand could be used without harmful effect on concrete strength. Cabrerae and al. [5] revealed also a correlation between the void content in mortar and the volume of paste required to start flowing such material.

Furthermore, the mineralogical source of crushed sands influence the concrete behaviour (with the same w/c ratio) as shown by Al-Ameeri [6] on three sands. The crushed sand from granite produced the best properties in term of compressive strength and workability. This behaviour has been attributed to the particular morphology of granite sand particles. Indeed, the texture and shape of the crushed sand particles have a great influence on the combination of cement paste and aggregates. The study concluded that crushed sand is a practical solution to limit the river sand exploitation, as long as the mechanical behaviour and the durability of concretes are not negatively impacted [7].

Based on such ideas, the aim of this study is to estimate the potential of crushed sands to replace alluvial sands, and to highlight the potential problem caused by this replacement for the purpose of better valorization. The study is carried out on three crushing sands and CEM II cement from Yaoundé (Cameroon). Physical, chemical and mineralogical characterization was carried out on sands while mechanical and microstructural tests were carried out on mortars. This work is part of the development of the use of crushing sands in the construction sector.

2 Materials and methods

2.1 Materials

2.1.1 Cement paste

The cement used in this study was a Portland cement NC CEM II of class 42.5 R with a fineness between 3900-4000 cm^2/g, and a density of 3.14 g/m^3. The cement came from the "Dangote company" located at Yaoundé (Cameroon). The chemical composition of cement determined by X-ray fluorescence (XRF) and its mineralogical composition are presented in Table 1 and Table 2, respectively. The water/cement (w/c) ratio was kept constant at 0.6 for all mortar's mixtures.

Table 1 : Chemical composition of the cement. LOI: loss on ignition at 1000 T°C

Elt	SiO_2	Al_2O_3	Fe_2O_3	MnO	MgO	CaO	Na_2O	K_2O	TiO_2	P_2O_5	LOI
(%)	25.99	7.23	6.35	0.13	2.56	48.91	1.02	0.91	0.97	0.26	2.67

Table 2 : Mineralogical composition of cement (composition given by the supplier).

Constituents	C_3S	C_2S	C_3A	C_4AF
Proportions (%)	50-65	15-20	≤ 7	≤ 5

2.1.2 Sands

Crushed sands whose characteristics are given in Table 3 and Table 4 came from three quarry aggregate mining sites in Yaoundé (Cameroon). The quarry operated by Arab Contractor, Gracam and Razel produced sands noted SA, SG and SR, respectively. The river sand came from the Sanaga River (running from north to south Cameroon) and it was noted SS. Petrographic analysis from thin slices of rock samples from the three quarries showed that rocks are all gneiss, with different textures and mineralogies. The fine fraction in sand, shown in Table 3, varies from 1.4% (SS) to 8.3% (SG). The fineness modulus remained quite similar for all sands (around 2,6). The sand equivalent (SE) test gives a SE percentage between 82.5 and 95.5%, reflecting the great cleanliness of sands, but with the risk of causing a defect in the plasticity of the concrete. [8].

Table 3. Fineness modulus and sand equivalent for tested crushed sands

Sand	Fines content (< 80 µm: %)	Fineness modulus	Sand equivalent (%)
SA	6.3	2.4	87.3
SG	8.3	2.7	89.9
SR	7.6	2.6	82.5
SS	1.4	2.6	95.9

Table 4. Chemical composition of crushed sand (%) from XRF (NF P 18-598). LOI: loss on ignition.

Sand	SiO_2	Al_2O_3	Fe_2O_3	MnO	MgO	CaO	Na_2O	K_2O	TiO_2	P_2O_5	LOI
SA	65.50	15.69	7.76	0.16	2.74	1.37	1.76	2.68	0.95	0.14	0.57
SG	62.55	16.61	8.81	0.19	3.18	1.68	1.84	2.68	1.00	0.17	0.41
SR	67.53	13.73	7.66	0.14	2.43	2.22	1.82	2.13	1.03	0.19	0.48
SS	90.16	3.96	1.54	0.03	0.08	0.23	0.43	2.01	0.23	--	0.79

The chemical composition of sands determined by X-ray fluorescence (XRF) in Table 4 showed similar compositions for all crushed sands. Sands are mainly siliceous with aluminum and iron. The proportions of aluminum and iron ($Fe_2O_3 + Al_2O_3$) are 23.45%, 25.42%, 21.39%, for SA, SG, SR, respectively, while this proportion reached only 5.5% for the river sand SS. The percentages of alkali equivalents (% Na_2O + 0.658% K_2O) are 3.84%, 3.89%, 3.33% and 2.29% for SA, SG, SR and SS, respectively. The crushed sands had a calcium content (CaO) around 7 times higher than river sand.

Figure 1 shows the diffractograms of crushed sands SA, SG, SR and river sand SS. The quantitative analysis of XRD patterns with TOPAS software (Rietveld method) showed that the river sand is essentially composed by quartz SiO_2 (85.6%), biotite $K(MgFe)_3(OH)_2(Si_3AlO_{10})$ (0.05%) and feldspars such as microcline $K(AlSi_3)O_8$ (10.6%) and albite $Na(Si_3Al)O_8$ (3.6%). The degree of crystallinity is about 87%. Similar crystalline phases were observed in crushed sands but they differ from river sand by the presence of a few additional phases. The average degree of crystallinity of the 3 crushed sands is around 96%. The main phases are quartz (57.2%), biotite (0.1%), mica (Annite) $Si_3AlO_{10}(OH)_2Al_2K$ (4.1%), Andesine $(Ca,Na)(Al,Si)_4O_8$ (4%), Almandine $Al_2Fe_3(SiO_4)_3$ (15.1%) and feldspars such as microcline (9.5%) and albite (9.7%). Such mineralogy is in accordance to the geological origin of sands (Gneiss). However the identification of traces of dolomite $CaMg(CO_3)_2$ (0.25%) is not in accordance with the geological identification of the rock.

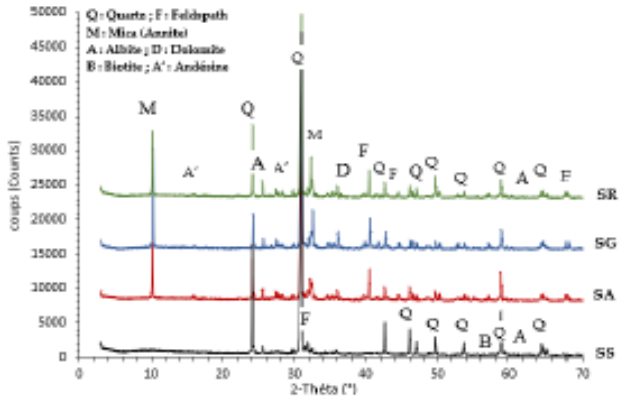

Fig. 1. XRD patterns of crushed sands SA, SG, SR and the river sand SS

2.2 Experimental program

2.2.1 Mixing procedure of mortars

The mixing procedure in this work is the Equivalent Concrete Mortar (ECM) method. Its principle is based on the existence of a simple correlation between the concrete rheological properties and the one of the mortar it contains [9]. It consists in replacing the granular skeleton with sand by keeping the same volume of cementitious paste and the same cement amount. We focused on the mixtures corresponding to mortars with 100%, 50% and 0% of SS and SR sands. The corresponding mortars are rated MSR100 (M: mortar, S: Sanaga sand, R: Razel sand, 100% Razel sand), MSR-50 (M: mortar, S: Sanaga sand, R: Razel sand, 50% Razel sand) and MSR-0 (M: mortar, S: Sanaga sand, R: Razel sand, 0% Razel sand), respectively. The w/c ratio 0.6 was similar for all the concretes while the CEM II/ B-P 42.5R cement content was fixed at 350kg/m^3. The compositions of mortars are given in Table 5.

Table 5. Compositions of manufactured mortars (for 1 m^3)

Component (kg/m^3)	MSR0	MSR50	MSR100
Crushed sand	0	918	1900
River sand	1771	918	0
Cement	350	350	350
Water	206	206	206

Using such formulation, prismatic specimens of mortar 40 x 40 x 160 mm have been made according to the EN 196-1 standard and tested after water immersion curing for 28 days. Results are the average of three tested specimens.

2.2.2 Testing methods

The compressive and bending strengths of mortars specimens were measured with a loading rate of 1.0 kN/s according to the NF P 18-406 standard. The water porosity test was carried out according to NF P 18-459 standard. The specimen was dried at 105°C at the end of the water porosity test and not initially as recommended in the standardized method. It allowed to lower the microstructural damage induced by high temperature.

The measurement of endogenous shrinkage was carried out on mortar samples according to the conditions described in standard NF P 18-427 and under climatic conditions at T=20±2°C and 50±5%RH.

X-ray diffraction (XRD) analyses were applied on sands and mortars ground to pass through a 80 µm sieve. Analyses were performed using a Bruker AXS D8 Advance diffractometer, in theta-theta geometry, equipped with a cobalt source (λ = 1.79 Å), without monochromator and a lynx Eye fast detector. Identification was done with EVA software coupled with ICDD Pdf2 mineralogical data base. The quantitative analyses were done with TOPAS software (Rietveld Analysis).

A thermal analyzer NETZSCH STA 409 E was used to collect the thermogravimetric curve (TG) and the derived thermogravimetric curve (DTA). Analyses allowed to evaluate the portlandite $Ca(OH)_2$, ettringite, C-S-H and calcium carbonate ($CaCO_3$) content in MSR0 and MSR100 mortars. The powder sample was heated from 20 to 1100 °C with a 10 °C/min heating rate under nitrogen to avoid carbonation during analysis.

The microstructure of mortars (after resin inclusion and polishing) was evaluated by Scanning Electron Microscope (SEM) using back scattered electrons mode. A chemical cartography was collected on polished surface by Energy Dispersive Spectroscopy (coupled with SEM). The morphology and the adhesion at paste/sand interface in mortars were evaluated [10].

3 Results and discussion

3.1 X-ray diffraction (XRD) on mortars

The XRD patterns of SR sand and mix-sand mortars MSR100 and MSR50 are presented on Fig. 2 while XRD patterns of SS sand and mix-sand mortars MSR0 and MSR50 are presented on Fig. 3.

The analysis shows that after cement addition, a few changes occurred on XRD patterns. Changes of peaks height may be due to a variation of the phase quantities (because of sands mixture, cement dilution or phase dissolution in alkaline medium) as well as a variation of particle aggregation. Indeed, the preferential orientation of phases during the filling of the XRD sample holder used is decreased in presence of cement paste.The preferential orientation mainly affects the sheet-formed phases becoming parallel to the plan of sample compaction in XRD sample holder. In presence of cement which allows the sheet dispersion and then their immobilization after hardening, the preferential orientation decreased inducing for example a decrease of annite peak at d = 10.09Å while its quantity may remain constant.

A small peak associated with portlandite (d=4.92Å) was observed as expected in the presence of Portland cement and the detection of crystalline or amorphous hydrates C-S-H remained difficult as shown by the zoomed view on Fig. 5 (a, b). Zoom represents the specific 2theta range for main XRD peaks of cementitious hydrates and calcite/dolomite. In the case of SR sand, the trace of calcite (d = 3.00/2.99Å) seemed to come from the sand itself (but its presence is not in accordance to the geology). Carbonation of the cement during curing occurred slightly with the development of a second peak associated to a new calcite form (d = 3.04Å), also present on SS river sand mortar. The formation of calcite comes from the carbonation of Portlandite $Ca(OH)_2$. Such phase is soluble in pore water and releases Ca^{2+} and OH^- ions. In the presence of CO_2 from the air, calcite may precipitate in such conditions. Calcite can also be obtained from the carbonation of cementitious hydrates that remain usually under amorphous state in a hardened cementitious paste. The change in the degree of crystallinity from TOPAS analysis also cannot help to detect an increase of amorphous product.

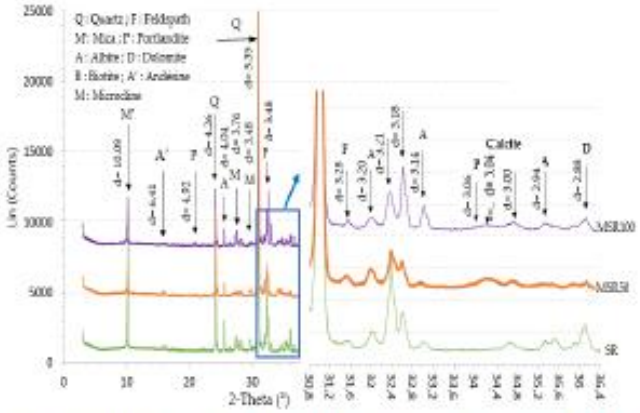

Fig. 2. XRD patterns of SR sand and mix-sand mortars MSR100 and MSR50

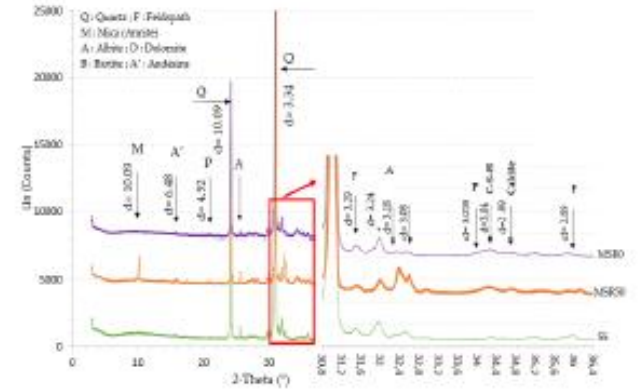

Fig. 3. XRD patterns of SS sand and mix-sand mortars MSR0 and MSR50

3.2 Water porosity

The water porosity values of mortars and the measuring system are presented in Fig. 4.

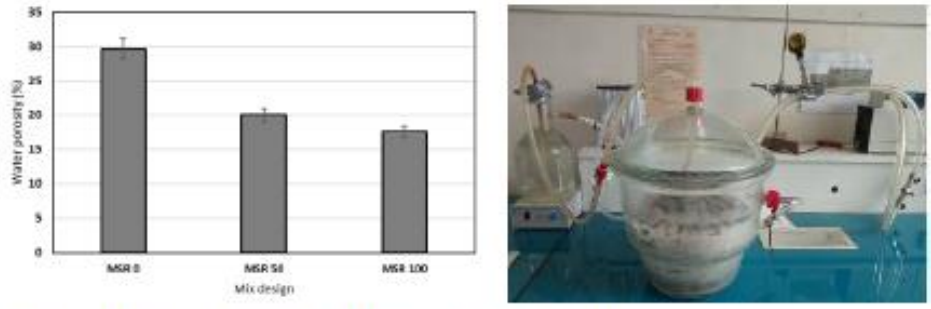

Fig. 4. a) The water porosity of different mortars, b) Sample saturation between measurement

The river sand mortar MSR0 showed a high porosity value (P = 29.7%) compared to the crushed sand mortar MSR100 (P = 18%). This difference was attributed to the low fine particle content in river sand (< 80µm = 1.4% against 6,5-8,5%). The mortar MSR50 manufactured with 50% of crushed sands presented an average porosity of 20% in Fig. 2. So, the presence of crushed sand in mortar decreased the water porosity, which is correlated to the improvement of compressive strength. On the other hand, the various formulations were made on the assumption of an identical w/c ratio, allowing a higher quantity of river sand and thus favouring a more interconnected porous structure.

3.3 Compressive strength and drying shrinkage

Figure 5 presents the compressive and bending strengths of mortars after 28 days curing in water.

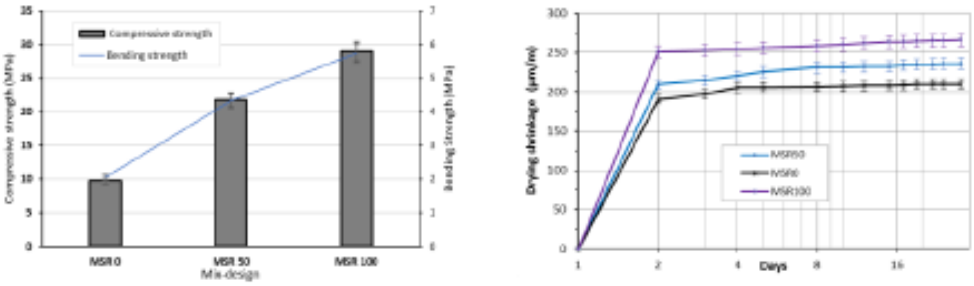

Fig. 5. Compressive strength and bending strength (a), drying shrinkage (b) measured on mortars

The results show that mortar containing only river sand has a very low compressive strength (Rc= 9.5±±0.4 MPa) compared to crushed sand mortars (Rc=20-30 MPa). This situation can be explained by the low content of fine particles in the river sand (< 80µm = 1.4%) compared to the crushed sands (<80µm=7.6%). Indeed, a high fine content is necessary for cohesion at the interface between the cement matrix and sand as well as for a low porosity. This average difference was about 7 MPa between 100% crushed sand mortars and 50/50 mixed sands mortars. The average compressive strength value was around 22 MPa for MSR50.

The shrinkage curves for all mortars show a small variation of the shrinkage after the second day of drying (same speed). It reflects the creation of voids within the matrix induced by the consumption of pore water, which induces a capillary depression within the system and thus a so-called self-dehydration deformation [11]., However, the MSR100 mortar has a greater shrinkage speed than the MSR0. The shrinkage is moderate for the MSR50 mortar.

3.4 Thermogravimetric analysis

The Fig. 6 (a, b) shows the TG curves and the differential thermal anlysis (DTA) for the mortars MSR0 and MSR100 after 92 days curing in water.

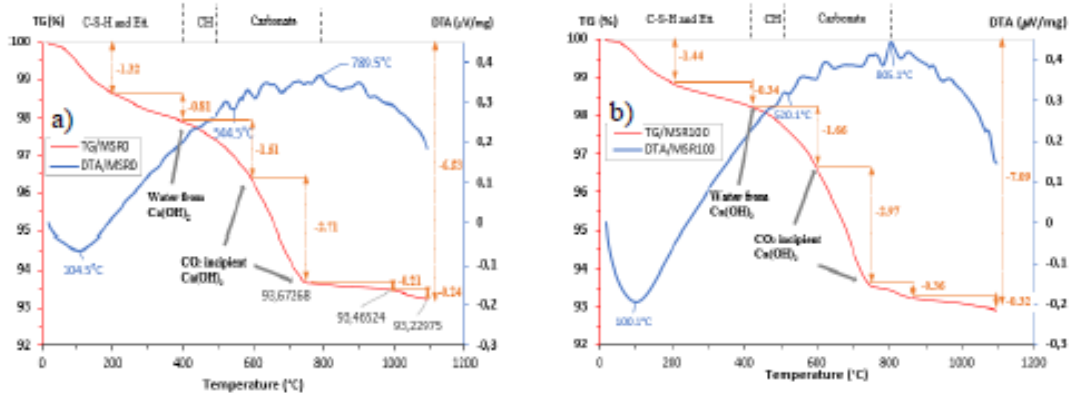

Fig.6. TG curves on MSR0 mortar (a) and MSR100 mortar (b).

The mass loss associated to each inflection points can be used to determine portlandite, C-S-H and calcite contents. For all analyses, the first mass loss between 20 and 400°C resulted mainly from the loss of free water and the dehydration of C-S-H and ettringite. The second mass loss around 460°C came from the decomposition of portlandite (CH). The third inflection point occurring between 600 and 800°C the consequence of the decarbonation of calcium carbonate ($CaCO_3$) produced by carbonation and other carbonated compounds [12]. The analysis shows that total mass losses or loss on ignition of MSR0 (LOI = 6.53%) and MSR100 (LOI = 7.09%) were similar. However, the mass losses at particular temperature appeared slightly different. The mass loss between 20 and 400°C

(dehydration of ettringite and CSH), between 410 and 480 °C (dehydration of CH) and between 580 and 750 °C (decarbonation) represented 1.32% and 0.81%, 2.71% (Fig.6a) for MSR0 mortar and 1.44%, 0.34%, 2.97% (Fig.6b) for MSR100 mortar. The carbonation of rived sand mortar is slightly higher than the one occurring in crushed sand mortar. It could be link to the higher porosity of the river sand mortar. The other phases (CSH, ettringite or portlandite) seemed to be similar whatever the nature of the sand and no negative effect seemed to appear.

3.5 Energy dispersive spectroscopic (EDX) analysis

The Fig.7 shows the EDX chemical mapping of silicon (Si) and calcium (Ca) on MSR0, MSR50 and MSR100 mortars after their inclusion into resin and polishing.

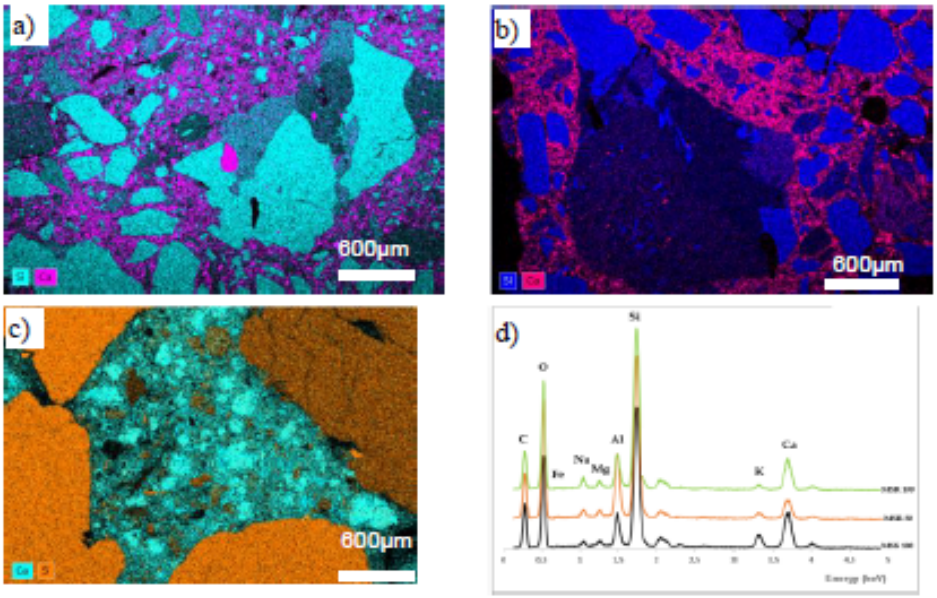

Fig.7. Silicon (Si) and calcium (Ca) mapping on mortar pastes (a) MSR100 (Si: blue, Ca: pink), (b) MSR50 (Si: blue, Ca: pink), (c) MSR0 (Ca: blue, Si: orange), (d) EDX spectra on concretes.

The 100% river sand mortar (Fig. 7c) showed silica aggregates (in orange) with irregular shapes, rounded angle and sizes ranging from 20 µm to several hundred micrometers, unlike 100% crushed sand mortars (Fig. 7 a). Crushed sand presented some angular particles (consequence of the crushing). The cement paste rich in calcium appeared in pink on Fig. 7a and b and in blue on Fig.7d and it filled the spaces between aggregates. The paste incorporated fine particles contained in crushed sands while the paste in 100% sand river mortar appeared more porous with non-homogeneous blue colour (the porosity appeared in black or dark blue in cement paste). In comparison, the cementitious matrix of the mixed sand mortars (Fig. 7 b) seemed more homogeneous with a better granular dispersion.

4 Conclusions

This study focused on the characterization of crushed sand and river sand as well as on their mixture in mortars. As a conclusion, the three tested crushed sands from Cameroon had a high proportion of fine particles (%), while the tested river sand presented a low fine content (%), which contributes to explain the difference of behaviour in mortars. Furthermore, thermogravimetric analysis (TG) revealed that the introduction of crushed sand didn't impact strongly the cementitious phases development. Ettringite, CSH or portlandite content from thermal analysis are similar in tested mortar while a slight difference of carbonation appeared with a lower carbonation in crushed sand that presented the lower water porosity (lower accessibility of CO_2 gas to the paste). Results are confirmed by XRD measurements showing the appearance of a small peak of calcite in mortar as well as portlandite.

The high fine content of the crushed sand does not have a negative influence on the compressive and bending strength of the mortars. MSR100 mortar has a high mechanical compressive strength compared to MSR0, moderate shrinkage is observed for the MSR50 mortar. Concerning the mortars

manufactured with sands mixtures, the compressive strength of hardened mortar is directly linked to the porosity. As expected, the compressive strength values of MSR50 mortars higher than 20 MPa proved that the mixture of river and crushed sands allowed the manufacture of mortars with satisfactory properties.

Results confirmed the ability to mix crushed sand with alluvial sand in the formulation of mortars, while increasing the mechanical strength and decreasing the water porosity. Now, this work has to be completed by durability test, especially the analysis of alkali-reaction.

Acknowledgements

This research work is part of a co-tutorship agreement between the CY Cergy Paris University (France) and the University of Yaoundé I (Cameroon). The authors gratefully acknowledge the financial support provided mainly by Campus France.

References

[1] M. L. K. Khouadjia, B. Mezghiche, et M. Drissi, « Experimental evaluation of workability and compressive strength of concrete with several local sand and mineral additions », *Construction and Building Materials*, vol. 98, p. 194‑203, nov. 2015, doi: 10.1016/j.conbuildmat.2015.08.081.

[2] L. Zeghichi, Z. Benghazi, et L. Baali, « The Effect of the Kind of Sands and Additions on the Mechanical Behaviour of S.C.C », *Physics Procedia*, vol. 55, p. 485‑492, janv. 2014, doi: 10.1016/j.phpro.2014.07.070.

[3] J. Dang et J. Zhao, « Influence of waste clay bricks as fine aggregate on the mechanical and microstructural properties of concrete », *Construction and Building Materials*, vol. 228, p. 116757, déc. 2019, doi: 10.1016/j.conbuildmat.2019.116757.

[4] B. Menadi, S. Kenai, J. Khatib, et A. Aït-Mokhtar, « Strength and durability of concrete incorporating crushed limestone sand », *Construction and Building Materials*, vol. 23, n° 2, p. 625‑633, févr. 2009, doi: 10.1016/j.conbuildmat.2008.02.005.

[5] O. A. Cabrera, L. P. Traversa, et N. F. Ortega, « Fluidez de morteros cementíceos con arenas machacadas », *Mater. construcc.*, vol. 60, n° 300, p. 115‑130, déc. 2010, doi: 10.3989/mc.2010.50909.

[6] A. Al-Ameeri, « using different types of fine aggregate to produce high strength concrete », International Journal of Arts & Sciences; Cumberland Vol. 5, N° 7, (2012): 187-196

[7] B. Benabed, E.-H. Kadri, L. Azzouz, et S. Kenai, « Properties of self-compacting mortar made with various types of sand », *Cement and Concrete Composites*, vol. 34, n° 10, p. 1167‑1173, nov. 2012, doi: 10.1016/j.cemconcomp.2012.07.007.

[8] « Sand Equivalent », *Pavement Interactive*. https://pavementinteractive.org/reference-desk/testing/aggregate-tests/sand-equivalent/ (consulté le avr. 04, 2020).

[9] S. Yang et H. Lee, « Mechanical properties of recycled aggregate concrete proportioned with modified equivalent mortar volume method for paving applications », *Construction and Building Materials*, vol. 136, p. 9‑17, avr. 2017, doi: 10.1016/j.conbuildmat.2017.01.029.

[10] K. L. Scrivener, « Backscattered electron imaging of cementitious microstructures: understanding and quantification », *Cement and Concrete Composites*, vol. 26, n° 8, p. 935‑945, nov. 2004, doi: 10.1016/j.cemconcomp.2004.02.029.

[11] M. Bouasker, « Étude numérique et expérimentale du retrait endogène au très jeune âge des pâtes de ciment avec et sans inclusions », thesis, Nantes, 2007.

[12] G. Villain, M. Thiery, et G. Platret, « Measurement methods of carbonation profiles in concrete: Thermogravimetry, chemical analysis and gammadensimetry », *Cement and Concrete Research*, vol. 37, n° 8, p. 1182‑1192, août 2007, doi: 10.1016/j.cemconres.2007.04.015.